AIP Advances

Low temperature activation of amorphous In-Ga-Zn-O semiconductors using microwave and e-beam radiation, and the associated thin film transistor properties

Cite as: AIP Advances **9**, 025204 (2019); https://doi.org/10.1063/1.5082862
Submitted: 25 November 2018 . Accepted: 30 January 2019 . Published Online: 11 February 2019

Seong Cheol Jang, Jozeph Park, Hyoung-Do Kim, Hyunmin Hong, Kwun-Bum Chung, Yong Joo Kim, and Hyun-Suk Kim

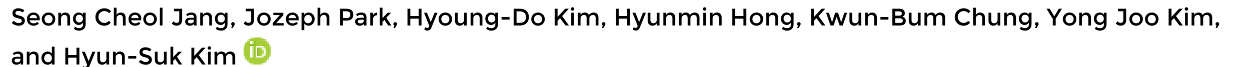

ARTICLES YOU MAY BE INTERESTED IN

Control of O-H bonds at a-IGZO/SiO_2 interface by long time thermal annealing for highly stable oxide TFT
AIP Advances **7**, 125110 (2017); https://doi.org/10.1063/1.5008435

Ultra-wide bandgap amorphous oxide semiconductors for NBIS-free thin-film transistors
APL Materials **7**, 022501 (2019); https://doi.org/10.1063/1.5053762

Metal oxide semiconductor thin-film transistors for flexible electronics
Applied Physics Reviews **3**, 021303 (2016); https://doi.org/10.1063/1.4953034

AIP Conference Proceedings
FLASH WINTER SALE!
50% OFF ALL PRINT PROCEEDINGS
ENTER CODE 50DEC19 AT CHECKOUT

AIP Publishing

© 2019 Author(s).

Low temperature activation of amorphous In-Ga-Zn-O semiconductors using microwave and e-beam radiation, and the associated thin film transistor properties

Cite as: AIP Advances 9, 025204 (2019); doi: 10.1063/1.5082862
Submitted: 25 November 2018 • Accepted: 30 January 2019 •
Published Online: 11 February 2019

Seong Cheol Jang,[1,a)] Jozeph Park,[2,a)] Hyoung-Do Kim,[1] Hyunmin Hong,[3] Kwun-Bum Chung,[3,b)] Yong Joo Kim,[4,c)] and Hyun-Suk Kim[1,d)]

AFFILIATIONS

[1] Department of Materials Science and Engineering, Chungnam National University, Daejeon 34134, Republic of Korea
[2] Department of Materials Science and Engineering, Korea Advanced Institute of Science and Technology, Daejeon 34141, Republic of Korea
[3] Division of Physics and Semiconductor Science, Dongguk University, Seoul 04620, South Korea
[4] Biosystems Machinery Engineering, Chungnam National University, Daejeon 34134, Republic of Korea

[a)] **Contributions:** These authors contributed equally to this work
[b)] **corresponding authors:** kbchung@dongguk;edu;
[c)] **corresponding authors:** babina@cnu.ac.kr
[d)] **corresponding authors:** khs3297@cnu.ac.kr

ABSTRACT

In-Ga-Zn-O (IGZO) films deposited by sputtering process generally require thermal annealing above 300°C to achieve satisfactory semiconductor properties. In this work, microwave and e-beam radiation are adopted at room temperature as alternative activation methods. Thin film transistors (TFTs) based on IGZO semiconductors that have been subjected to microwave and e-beam processes exhibit electrical properties similar to those of thermally annealed devices. However spectroscopic ellipsometry analyses indicate that e-beam radiation may have caused structural damage in IGZO, thus compromising the device stability under bias stress.

© 2019 Author(s). *All article content, except where otherwise noted, is licensed under a Creative Commons Attribution* (CC BY) *license* (*http://creativecommons.org/licenses/by/4.0/*). https://doi.org/10.1063/1.5082862

Amorphous silicon (*a*-Si) has been the most commonly used semiconductor material for thin film transistors (TFTs) in the field of flat panel displays for the past many decades. However, its field effect mobility is limited to less than 1 cm^2/Vs, and stability can be a problem in some applications.[1] Amorphous oxide semiconductors (AOSs) have attracted considerable attention as possible substitutes owing to their high carrier mobility and areal uniformity.[2–4] The oxide semiconductor material that is already available in the market is amorphous In-Ga-Zn-O (a-IGZO), which is implemented in TFT backplanes of liquid crystal displays (LCDs) or organic light emitting diode (OLED) panels.[5,6] Devices based on IGZO semiconductor exhibit relatively high field-effect mobility (>10 cm^2/Vs) compared to their a-Si counterparts.[7] To deposit a-IGZO, magnetron sputtering is commonly used. However, the fabrication of IGZO TFTs with reasonably good electrical performance usually requires thermal annealing at temperatures near 300°C.[8,9] Many research group aim at decreasing the annealing temperature to enable the fabrication of devices on plastic substrates, so that flexible displays may be realized in a cost effective way.[10–12]

In this work, microwave and electron beam (e-beam) radiation methods are adopted to reduce the treatment temperature for the activation of IGZO TFTs. It is shown that

© Author(s) 2019

reasonable TFT performance may be obtained by both methods, however e-beam annealing appears to cause structural damage in the IGZO layers, resulting in devices that are more susceptible to degradation upon bias stress.

IGZO TFTs with an inverted staggered bottom gate structure were fabricated on highly doped p-type Si substrates with thermally grown 100 nm-thick SiO_2 layers. The highly doped p-type Si and 100 nm SiO_2 were used as the gate electrode and gate insulator, respectively. 30 nm-thick IGZO films were deposited by radio frequency (RF) magnetron sputtering using a 3-inch IGZO target with an atomic composition ratio of In:Ga:Zn = 1:1:1. The plasma gas used was Ar, at a flow rate of 20 sccm. The working pressure was maintained at 7 mTorr and an RF power of 100 W was applied to the IGZO target. After performing the annealing treatment on the IGZO film, a 150-nm thick indium tin oxide (ITO) film was deposited and patterned to form the source/drain electrodes, using shadow masks. The channel width and length of the IGZO devices were 800 and 200 μm, respectively.

The microwave annealing of IGZO layers was performed at a power and frequency of 600 W and 2.45 GHz, respectively. Microwave radiation was applied for 1 hour in air ambient. In general, ZnO-based materials can absorb the electromagnetic wave energy in frequency range of 2 to 18 GHz.[13] Therefore, it is anticipated that IGZO will absorb the microwave energy at the frequency applied in this work. For e-beam annealing, an electron beam with an energy and current of 0.2 MeV and 10 mA, respectively. Here the duration was varied from 3 to 10 minutes in air. Additionally, a reference IGZO TFT with a typical thermal annealing process was fabricated for comparison. The thermal annealing was conducted in a conventional rapid thermal annealing system in air ambient for 1 hour at 300 °C.

The crystal structures of the IGZO films were examined by grazing incidence angle X-ray diffraction (XRD; Rigaku, D/MAX2500, Cu Kα radiation). The diffraction patterns of the samples were taken in the 2θ range from 20 to 80° with a step size of 0.05°. The chemical bonding states were examined using X-ray photoelectron spectroscopy (XPS) using a monochromatic Mg Kα (1253.6 eV) source and a pass energy of 50 eV.

The electrical characteristics of TFTs were evaluated in the dark at room temperature using an HP 4156B semiconductor parameter analyzer, under air ambient conditions. The field-effect mobility was extracted in the saturation regime with the drain voltage (V_D) fixed at 10 V. The devices were subjected to negative bias stress (NBS), positive bias stress (PBS) and negative bias illumination stress (NBIS). For NBS and NBIS, the gate voltage (V_G) and drain voltage (V_D) applied were -20 and 0.1 V, respectively. A light source with a luminance of 1500 lux was used to illuminate the devices from the top during NBIS. For PBS, the applied V_G and V_D were 20 and 0.1 V, respectively. Each stress test was conducted in air at room temperature for 1 hr.

The transfer characteristics of IGZO films are shown in Figure 1. Table I consists of representative parameters such as saturation filed effect mobility (μ_{sat}), threshold voltage (V_{th}) and subthreshold swing (SS). Metallic behavior was

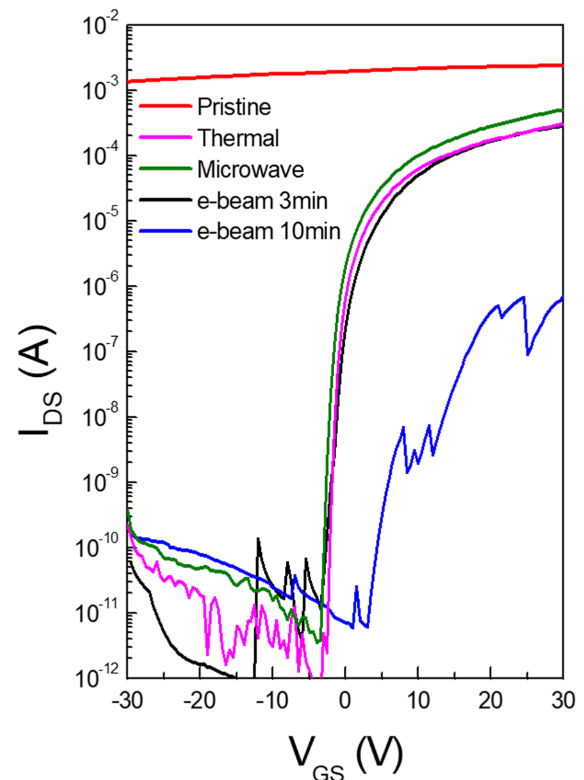

FIG. 1. Representative transfer characteristics of the IGZO TFTs with the active layer subjected to different annealing processes.

observed in the pristine TFTs fabricated without annealing, which implies that a relatively high carrier concentration is present in the IGZO layer. Semiconducting properties could be obtained after thermal, microwave, and e-beam treatment. Thermally annealed IGZO TFTs exhibit μ_{sat}, V_{th}, and SS values of 8.10 cm^2/Vs, -1.34 V and 0.32 V/decade, respectively. Increased field effect mobility (11.3 cm^2/Vs) is observed in devices fabricated with microwave annealed IGZO, accompanied with a slight negative shift of the initial V_{th} value (-1.54 V). Devices that have been exposed to 3 min e-beam annealing exhibit relatively low mobility (7.40 cm^2/Vs) with slightly negative V_{th} (-1.95 V) values. As the e-beam annealing time is increased to 10 minutes, extremely low performance is obtained, as shown in Figure 1.

TABLE I. Device parameters of the IGZO TFTs, including the μ_{sat}, S.S., V_{th}, and I_{on}/I_{off} ratio values, with respect to different annealing processes.

Annealing Type	μ_{sat} (cm^2/Vs)	S.S (V/dec)	V_{th} (V)	I_{on}/I_{off}
Pristine		N/A		
Thermal	8.10	0.24	-1.34	10^9
Microwave	11.25	0.32	-1.54	10^9
e-beam 3min	7.40	0.60	-1.95	10^9
e-beam 10min		N/A		

© Author(s) 2019

TABLE II. ΔV_{th} values under NBS, PBS, NBIS, for the IGZO TFTs with respect to different annealing processes.

Annealing Type	Thermal	Microwave	e-beam
	NBS		
ΔV_{th} (V)	−0.38	−0.57	−1.08
	PBS		
ΔV_{th} (V)	0.6	0.54	0.99
	NBIS		
ΔV_{th} (V)	−0.1	−0.3	−6.86

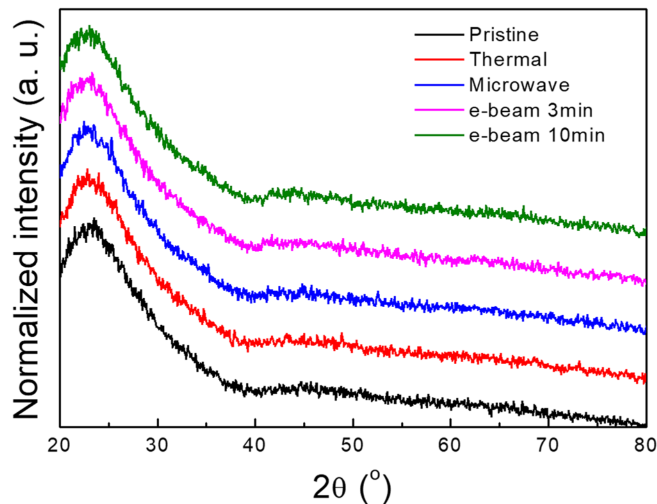

FIG. 2. Grazing incidence angle X-ray diffraction (GIAXRD) patterns of IGZO TFTs with respect to different annealing processes.

To evaluate the stability of IGZO TFTs, negative bias stress (NBS), positive bias stress (PBS), and negative bias illumination stress (NBIS) tests were conducted on three samples, each having been subjected to thermal, microwave, and 3-min e-beam annealing. The results are summarized in Table II. As the stress time increases, all IGZO TFTs undergo negative (NBS, NBIS) and positive (PBS) shifts in V_{th}. While the devices fabricated with microwave and thermal annealing undergo relatively small shifts in threshold voltage ($|V_{th}| < 1$ V) under all stress conditions, those having been subjected to e-beam annealing exhibit rather poor stability with ΔV_{th} values of -1.08, 0.99, and -6.86 V under NBS, PBS, and NBIS, respectively. At this point it may be anticipated that a high concentration of defects acting as charge traps is present in the IGZO film exposed to e-beam radiation.

X-ray diffraction (XRD) and atomic force microscopy (AFM) analyses were carried out to examine the microstructure of the IGZO films annealed under different conditions. Figure 2 shows the diffraction patterns of each type of IGZO films appear to be amorphous regardless of the annealing process. This indicates that both microwave and e-beam radiation used in the present study do not crystallize the IGZO films. The AFM surface topography images are shown in Figure 3. Compared with the pristine IGZO film (0.12 nm), the surface roughness increases with thermal annealing (0.28 nm). Microwave annealed IGZO has a lower root mean square (RMS) roughness value (0.19 nm) than those of e-beam annealed IGZO layers (0.44 and 0.83 nm for 3-min and 10-min e-beam radiation, respectively). The above results imply that as the thermal budget increases, the surface roughness increases, and may be indicative of the overall defect density in the IGZO film.

XPS analyses were performed to analyze the chemical bonding states of oxygen anions in the annealed IGZO layers. Figure 4 shows the O 1s peak spectra of each film. Peaks were

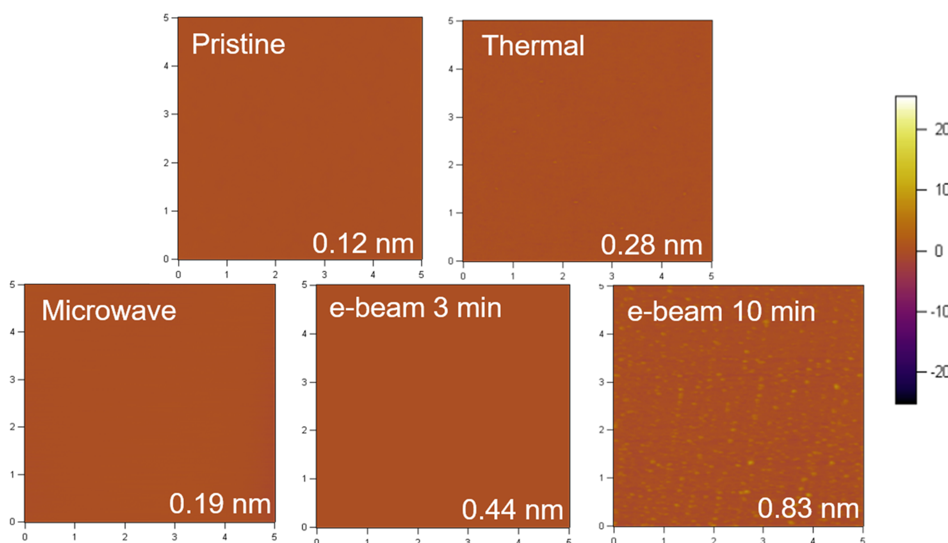

FIG. 3. Atomic force microscope topography images of IGZO films with respect to different annealing processes.

© Author(s) 2019

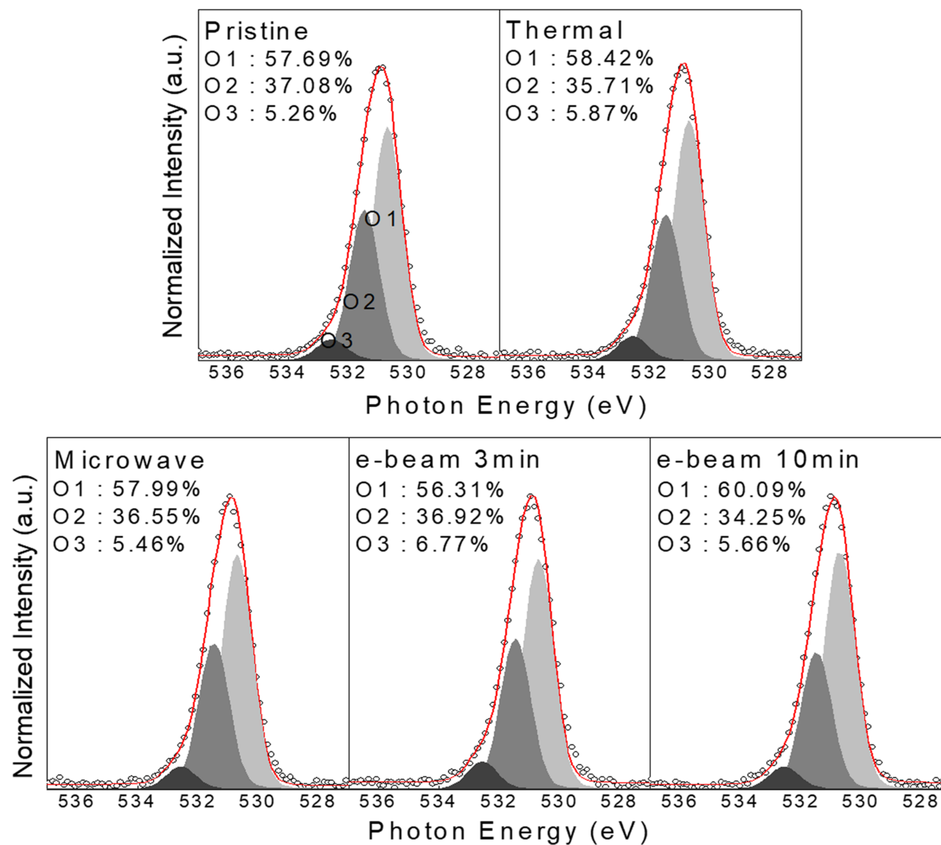

FIG. 4. XPS O 1s spectra of IGZO films with respect to different annealing processes.

resolved as the sum of three sub-peaks, centered at 530.7 eV (O1), 531.4 eV (O2), and 532.5 eV(O3). The sub-peak O1 is related to oxygen ions forming metal-oxide bonds, while peak O2 originates from oxygen anions near oxygen vacant sites, and peak O3 is related to hydroxyl groups in the IGZO films.[14] In oxide semiconductors, oxygen deficiency is strongly related to the generation of free carriers,[15] therefore sub-peak O2 is generally used to estimate the concentration of oxygen related defects and free carriers. All annealing processes result in decreased sub-peak O2 area, which is indicative of decreasing free carrier density, thus inducing relatively positive initial V_{th} values.

Figure 5(a) shows the refractive indices (R-value) as a function of photon energy, extracted from spectroscopic ellipsometry (SE), which may reflect the structural density of the films. Generally, dense layers exhibit relatively high R-values.[16,17] Compared to the pristine IGZO, the samples that have been subjected to thermal and microwave annealing exhibit higher R-values over the entire photon energy range (1 to 5 eV). On the other hand, e-beam annealing appears to reduce the R-values considerably. This suggests that the relatively rapid e-beam treatment induces structural modifications within the IGZO layer, while the time for rearrangement is not sufficient. Figure 5(b) shows the extinction coefficients, also extracted from the SE spectra. The optical band gap values can be extrapolated using the Tauc method, as shown in the equation below:[18]

$$(\alpha h\nu)^{1/2} = A(h\nu - E_g)$$

where h is Planck constant, ν the photon frequency, α the absorption coefficient, E_g the band gap, and A a proportionality constant. The band gap values are summarized in Table III. All annealing processes result in increased optical bandgap.

Figure 5(c) shows the band edge states below the conduction band minimum of each IGZO films, extracted from the imaginary dielectric functions. The fitted Gaussian peaks represent unoccupied trap states within the forbidden gap. The band edge state below the conduction band may be resolved into a shallow band edge state (D1) and a deep band edge state (D2), which are located at 3.18 and 2.56 eV from the valence band maximum, respectively. Shallow band edge states are related to the free carrier concentration, while deep band states reflect the amount of defects that act as traps of scattering centers.[19] In oxide semiconductor, the carrier mobility is generally proportional to the free carrier concentration.[20] In addition, trapping or scattering of carriers are most likely to be associated with the degradation of TFT devices under bias stress. The sub-area peak ratios of the D1 and D2 states are summarized in Figure 5(d). The number of shallow band

© Author(s) 2019

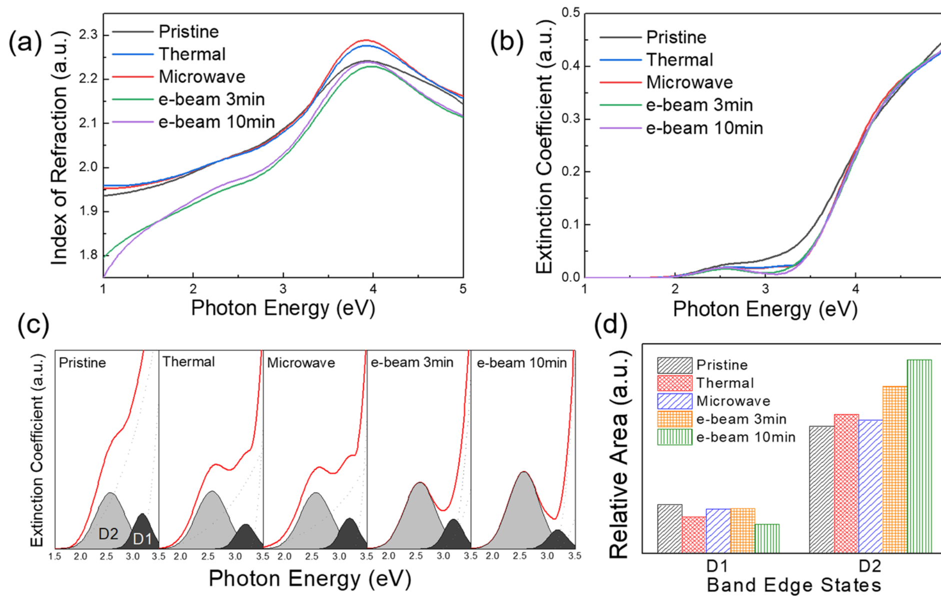

FIG. 5. (a) Index of refraction and (b) extinction coefficient and (c) enlargement of band edge states below the conduction band minima of the IGZO films with respect to different annealing processes, measured by spectroscopic ellipsometry (SE). (d) Relative sub-peak areas of the D1 and D2 states in IGZO, with respect to the different annealing processes.

edge states (D1) appears to decrease under all annealing processes compared to the pristine IGZO, resulting in positive shifts in the initial V_{th} in the associated TFTs. The relative area of D1 states is smallest after 10 min e-beam annealing, which indeed results in the poorest TFT performance. Microwave and 3 min e-beam annealing have similar D1 sub-peak area, however the D2 portion is larger in the latter, which may account for the more pronounced degradation of the corresponding TFT under bias stress. Here the D2 states are anticipated to act as charge traps, thus causing relatively large V_{th} shifts upon prolonged bias stress. Such defects are highly likely to be generated by the physical energy of the e-beam, which may induce structural damage within the IGZO layers. It is therefore necessary to optimize a balance between the total thermal budget and physical damage induced in the semiconductor, in order to lower the process temperature for the fabrication of IGZO TFTs. Here, microwave annealed devices exhibit the best performance and stability, owing to the conversion of microwave energy into thermal energy without causing structural damage.

In the present study, effects of microwave and e-beam annealing on IGZO films and their corresponding TFTs have been investigated. The IGZO TFTs fabricated by microwave annealing exhibit a typical field effect mobility of 11.3 cm^2/Vs and a threshold voltage of -1.54 V. The devices subjected to e-beam annealing exhibit a slightly lower mobility of 7.40 cm^2/Vs and a more negative threshold voltage of -1.95 V. Both annealing processes activate the IGZO active layer successfully at room temperature. As a reference, it is shown that thermally annealed IGZO TFTs exhibit μ_{sat} and V_{th} values of 8.10 cm^2/Vs and -1.34 V, respectively. IGZO TFTs fabricated by thermal and microwave annealing exhibit good performance and stability throughout NBS, PBS, NBIS. On the other hand, while similar performance may be obtained by e-beam annealing, the stability appears to be compromised, especially in the presence of light (NBIS). Thin film analyses suggest that structural damage is induced during e-beam radiation, which generate electrical defect levels within the forbidden bandgap of IGZO. The latter are manifested as band edge states in the spectroscopic ellipsometry results.

TABLE III. Optical band gap values of IGZO films with respect to different annealing processes, extracted using the Tauc method.

Annealing Type	Band gap (eV)
Pristine	3.25
Thermal	3.41
Microwave	3.42
e-beam 3min	3.40
e-beam 10min	3.39

This work was supported by Basic Science Research Program through the National Research Foundation of Korea (NRF) funded by the Ministry of Education (Grant No: NRF-2017R1D1A1B03032375) and also by the MOTIE (Ministry of Trade, Industry & Energy (Grant No: 10051403)) and KDRC (Korea Display Research Corporation) support program for the development of future devices technology for display industry.

The authors declare no competing financial interest.

REFERENCES

[1] Y. Ye, R. Lim, and J. M. White, "High mobility amorphous zinc oxynitride semiconductor material for thin film transistors," J. Appl. Phys. **106**, 074512 (2009).

[2] K. Nomura, H. Ohta, A. Takagi, T. Kamiya, M. Hirano, and H. Hosono, "Room-temperature fabrication of transparent flexible thin-film transistors using amorphous oxide semiconductors," Nature **432**, 488–492 (2004).

© Author(s) 2019

[3]A. Nathan, S. Lee, S. Jeon, and J. Robertson, "Amorphous oxide semiconductor TFTs for displays and imaging," J. Display Technol. **10**, 917–927 (2014).

[4]H. Hosono, "Ionic amorphous oxide semiconductors: Material design, carrier transport, and device application," J. Non-Crys. Solids **352**, 851–858 (2006).

[5]J. H. Lee, D. H. Kim, D. J. Yang, S. Y. Hong, K. S. Yoon, P. S. Hong, C. O. Jeong, H. S. Park, S. Y. Kim, S. K. Lim, S. S. Kim, K. S. Son, T. S. Kim, J. Y. Kwon, and S. Y. Lee, "World's largest (15-inch) XGA AMLCD panel using IGZO oxide TFT," SID Int. Symp. Dig. Tech. Pap. **39**, 625–628 (2008).

[6]J. K. Jeong, J. H. Jeong, J. H. Choi, J. S. Im, S. H. Kim, H. W. Yang, K. N. Kang, K. S. Kim, T. K. Ahn, H. J. Chung, M. Kim, B. S. Gu, J. S. Park, Y. G. Mo, H. D. Kim, and H. K. Chung, "12.1-inch WXGA AMOLED display driven by indium-gallium-zinc oxide TFTs array," SID Int. Symp. Dig. Tech. Pap. **39**, 1–4 (2008).

[7]C. C. Lo and T. E. Hsieh, "Preparation of IGZO sputtering target and its applications to thin-film transistor devices," Ceram. Int. **38**, 3977–3983 (2012).

[8]Y. J. Tak, B. D. Ahn, S. P. Park, S. J. Kim, A. R. Song, K. B. Chung, and H. J. Kim, "Activation of sputter-processed indium–gallium–zinc oxide films by simultaneous ultraviolet and thermal treatments," Sci Rep **6**, 21869 (2016).

[9]D. G. Yang, H. D. Kim, J. H. Kim, K. Park, J. H. Kim, Y. J. Kim, J. Park, and H. S. Kim, "Performance and stability of amorphous In-Ga-Zn-O thin film transistors involving gate insulators synthesized at low temperatures," J. Alloy. Compd. **729**, 1195–1200 (2017).

[10]H. Lee, K. S. Chang, Y. J. Tak, T. S. Jung, J. W. Park, W. G. Kim, J. Chung, C. B. Jeong, and H. J. Kim, "Electric field-aided selective activation for indium-gallium-zinc-oxide thin film transistors," Sci Rep **6**, 35044 (2016).

[11]Y. J. Tak, S. P. Park, T. S. Jung, H. Lee, W. G. Kim, J. W. Park, and H. J. Kim, "Reduction of activation temperature at 150°C for IGZO films with improved electrical performance via UV-thermal treatment," J. Inf. Disp. **17**, 73–78 (2016).

[12]M. G. Stanford, J. H. Noh, K. Mahady, A. V. Ievlev, P. Maksymovych, O. S. Ovchinnikova, and P. D. Rack, "Room temperature activation of InGaZnO thin-film transistors via He^+ irradiation," ACS Appl. Mater. Inter. **9**, 35125–35132 (2017).

[13]L. F. Teng, P. T. Liu, Y. J. Lo, and Y. J. Lee, "Effects of microwave annealing on electrical enhancement of amorphous oxide semiconductor thin film transistor," Appl. Phys. Lett. **101**, 132901 (2012).

[14]J. H. Park, Y. Kim, S. Yoon, S. Hong, and H. J. Kim, "Simple method to enhance positive bias stress stability of In–Ga–Zn–O thin-film transistors using a vertically graded oxygen-vacancy active layer," ACS Appl. Mater. Interfaces **6**, 21363–21368 (2014).

[15]J. S. Park, W. J. Maeng, H. S. Kim, and J. S. Park, "Review of recent developments in amorphous oxide semiconductor thin-film transistor devices," Thin Solid Films **520**, 1679–1693 (2012).

[16]K. Sangwal and W. Kucharczyk, "Relationship between density and refractive index of inorganic solids," J. Phys. D **20**, 522 (1987).

[17]J. H. Kim, C. O. Chung, D. Sheen, Y. S. Sohn, H. C. Sohn, J. W. Kim, and S. W. Park, "Effect of fluorine incorporation on silicon dioxide prepared by high density plasma chemical vapor deposition with $SiH_4/O_2/NF_3$ chemistry," J. Appl. Phys. **96**, 1435 (2004).

[18]V. M. Bhuse, P. P. Hankare, K. M. Garadkar, and A. S. KHomane, "A simple, convenient, low temperature route to grow polycrystalline copper selenide thin films," Mater. Chem. Phys. **80**, 82–88 (2003).

[19]H. W. Park, A. Song, S. Kwon, D. Choi, Y. Kim, B. H. Jun, H. K. Kim, and K. B. Chung, "Enhancing the performance of tungsten doped InZnO thin film transistors via sequential ambient annealing," Appl. Phys. Lett. **112**, 123501 (2018).

[20]J. Y. Kwon, D. J. Lee, and K. B. Kim, "Transparent amorphous oxide semiconductor thin film transistor," Electron. Mater. Lett. **7**, 1–11 (2011).

© Author(s) 2019